J|A|C|S
ARTICLES

Published on Web 08/03/2010

Design and Synthesis of Vanadium Hydrazide Gels for Kubas-Type Hydrogen Adsorption: A New Class of Hydrogen Storage Materials

Tuan K. A. Hoang,[†] Michael I. Webb,[§] Hung V. Mai,[†] Ahmad Hamaed,[†] Charles J. Walsby,[§] Michel Trudeau,[‡] and David M. Antonelli*[,#]

Department of Chemistry and Biochemistry, University of Windsor, 401 Sunset Avenue, Windsor, Ontario N9B 3P4, Canada, Department of Chemistry, Simon Fraser University, 8888 University Drive, Burnaby, British Columbia V5A 1S6, Canada, Emerging Technologies, Hydro-Québec Institute, 1800 Boul. Lionel-Boulet, Varennes, Quebec J3X 1S1, Canada, and Sustainable Environment Research Center, University of Glamorgan, Pontypridd CF37 1DL, United Kingdom

Received June 5, 2010; E-mail: dantonel@glam.ac.uk

Abstract: In this paper we demonstrate that the Kubas interaction, a nondissociative form of weak hydrogen chemisorption with binding enthalpies in the ideal 20−30 kJ/mol range for room-temperature hydrogen storage, can be exploited in the design of a new class of hydrogen storage materials which avoid the shortcomings of hydrides and physisorpion materials. This was accomplished through the synthesis of novel vanadium hydrazide gels that use low-coordinate V centers as the principal Kubas H_2 binding sites with only a negligible contribution from physisorption. Materials were synthesized at vanadium-to-hydrazine ratios of 4:3, 1:1, 1:1.5, and 1:2 and characterized by X-ray powder diffraction, X-ray photoelectron spectroscopy, nitrogen adsorption, elemental analysis, infrared spectroscopy, and electron paramagnetic resonance spectroscopy. The material with the highest capacity possesses an excess reversible storage of 4.04 wt % at 77 K and 85 bar, corresponding to a true volumetric adsorption of 80 kg H_2/m^3 and an excess volumetric adsorption of 60.01 kg/m^3. These values are in the range of the ultimate U.S. Department of Energy goal for volumetric density (70 kg/m^3) as well as the best physisorption material studied to date (49 kg H_2/m^3 for MOF-177). This material also displays a surprisingly high volumetric density of 23.2 kg H_2/m^3 at room temperature and 85 bar — roughly 3 times higher than that of compressed gas and approaching the DOE 2010 goal of 28 kg H_2/m^3. These materials possess linear isotherms and enthalpies that rise on coverage and have little or no kinetic barrier to adsorption or desorption. In a practical system these materials would use pressure instead of temperature as a toggle and can thus be used in compressed gas tanks, currently employed in many hydrogen test vehicles, to dramatically increase the amount of hydrogen stored and therefore the range of any vehicle.

Introduction

Hydrogen is an ideal fuel because it is clean and renewable and possesses the highest amount of energy per gram of any chemical substance. However, the storage of hydrogen still remains elusive.[1] Some metal hydrides[2] contain enough hydrogen to satisfy the 2015 gravimetric (5.5 wt %) and volumetric (60 kg/m^3) targets established by the U.S. Department of Energy (DOE); however, sluggish kinetics and problems due to high enthalpies of adsorption (70 kJ/mol) necessitate exotic engineering solutions that substantially lower these values in any practical system. In contrast, physisorption materials[3] adsorb up to 7.5 wt % of hydrogen at 77 K with heats of adsorption in the range of 4−13 kJ/mol H_2,[4] but cooling to cryogenic temperatures dramatically cuts into the efficiency of this technology. Because of the limitations of these technologies, researchers have begun to explore the potential of the Kubas

[†] University of Windsor.
[§] Simon Fraser University.
[‡] Hydro-Québec Institute.
[#] University of Glamorgan.

(1) (a) Schlapbach, L.; Zuettel, A. *Nature* **2001**, *414*, 353–358. (b) Seayad, A. M.; Antonelli, D. M. *Adv. Mater.* **2004**, *16*, 765. (c) Yaghi, O. M.; O'Keeffe, M.; Ockwig, N. W.; Chae, H. K.; Eddaoudi, M.; Kim, J. *Nature* **2003**, *423*, 705. (d) Mark Thomas, K. *Dalton Trans.* **2009**, 1487–1505. (e) Yang, R. T.; Wang, Y. *J. Am. Chem. Soc.* **2009**, *131*, 4224. (f) Lochan, R. C.; Head-Gordon, M. *Phys. Chem. Chem. Phys.* **2006**, *8*, 1357. (g) Eberle, U.; Felderhoff, M.; Schueth, F. *Angew. Chem., Int. Ed.* **2009**, *48*, 2.

(2) (a) Orimo, S.; Nakamori, Y.; Eliseo, J. R.; Zuettel, A.; Jensen, C. M. *Chem. Rev.* **2007**, *107*, 4111–4132. (b) Sandrock, G. *J. Alloys Compd.* **1999**, *293*, 877.

(3) (a) Wong-Foy, A. G.; Matzger, A. J.; Yaghi, O. M. *J. Am. Chem. Soc.* **2006**, *128*, 3494. (b) Dailly, A.; Vajo, J. J.; Ahn, C. C. *J. Phys. Chem. B* **2006**, *110*, 1099. (c) Panella, B.; Hirscher, M.; Pütter, H.; Müller, U. *Adv. Funct. Mater.* **2006**, *16*, 520. (d) Langmi, H. W.; Book, D.; Walton, A.; Johnson, S. R.; Al-Mamouri, M. M.; Speight, J. D.; Edwards, P. P.; Harris, I. R.; Anderson, P. A. *J. Alloys Compd.* **2005**, *404−406*, 637. (e) Kaye, S. S.; Long, J. R. *J. Am. Chem. Soc.* **2005**, *127*, 6506. (f) Strobel, R.; Garche, J.; Moseley, P. T.; Jorissen, L.; Wolf, G. *J. Power Sources* **2006**, *159*, 781. (g) Hirscher, M.; Panella, B. *Scr. Mater.* **2007**, *56*, 809. (h) Hirscher, M.; Panella, B. *Scr. Mater.* **2007**, *56*, 803. (i) Yan, Y.; Lin, X.; Yang, S.; Blake, A. J.; Dailly, A.; Champness, N. R.; Hubberstey, P.; Schroeder, M. *Chem. Commun.* **2009**, 1025.

(4) Vitillo, J. G.; Regli, L.; Chavan, S.; Ricchiardi, G.; Spoto, G.; Dietzel, P. D. C.; Bordiga, S.; Zecchina, A. *J. Am. Chem. Soc.* **2008**, *130*, 8386.

 10.1021/ja104926h

interaction, a nondissociative weak form of hydrogen chemisorption that relies on strong back-donation of electron density into the H−H antibonding orbital.[5−9] Calculations by Zhao et al.[7] and Yildirim et al.[10] demonstrated that this approach is viable using systems containing a high concentration of low-coordinate early transition metal species in low oxidation states with ideal heats of adsorption within the range of 20−30 kJ/mol H_2. In this regard, many high surface area materials, including manganese-containing metal−organic framework materials,[11] in which one Mn can bind up to one H_2, have been studied. Silica-supported organotitanium(III)[12] and organochromium[13] species which adsorb up to an average of 3.8 and 2.2 H_2 per metal atom, respectively, at 77 K and 60 bar, with enthalpies in the 18−23 kJ/mol range, have also been studied. Because of these higher enthalpies, up to 41% of the adsorption at the Ti center is retained at 298 K, corresponding to 1.8 H_2/Ti. However, the active metal in these systems corresponds to at most 5% of the total weight, making the contribution from the Kubas interaction negligible. For this reason we chose to fabricate new extended solids using a small and light linker group to bridge coordinatively unsaturated metal centers capable of binding H_2. Hydrazine is the ideal linker because it is large enough to keep the metal centers apart and prevent clustering yet also small enough to minimize void space, which decreases volumetric performance. The hypothetical microporous solid MN_2H_x (M = Cr, V, Ti) should hold roughly 5% H_2 at room temperature based on 1.8 H_2 per metal, on the basis of the molecular weight and the best results observed in the silica-supported systems. These microporous solids have a high density of transition metal centers which are capable of forming Kubas interactions with appropriate energy. Thus, by analogy to the protolysis reaction of trimethylaluminium with hydrazine to yield an amorphous aluminum hydrazide gel,[14] we hypothesized that the reaction of a low-valent, low-coordinate early transition metal alkyl complex possessing bulky ligands to stabilize the low coordination number, with just enough hydrazine to eliminate the alkyl groups and bridge the transition metals, should create a microporous network in which the metal centers are kinetically "frozen" into an unusually low coordination state capable of binding H_2. Using this method, a cyclopentadienyl chromium hydrazide gel was recently synthesized in our group that possesses a low specific surface area of 32 m^2/g but adsorbs up to 1.75 wt % of hydrogen at 77 K and 80 bar.[15] The most exciting feature of this material is that 49% of the 77 K adsorption capacity is retained at room temperature, as compared to less than 15% for physisorption materials. This is because of the high adsorption enthalpies, which rise from 10 to 45 kJ/mol with adsorption. While these materials were a step forward in many ways, the Cr centers still retained one cyclopentadienyl group, essentially limiting the activity by shutting down three coordination sites per metal that could be used as binding sites for dihydrogen. In this work, trismesitylvanadium(III) was chosen as a precursor because of its ease of synthesis, low coordination number, and the ability of V(III) to back-bond to the H−H antibonding orbital. Previous results from our group also showed that vanadium(III) organometallic fragments grafted on silica coordinate 2.68 and 0.37 H_2/V at 80 bar and 77 or 298 K, respectively.[16] Mesitylene ligands are also more readily eliminated by protolysis reactions than cyclopentadienyl groups and should thus allow for a greater concentration of Kubas binding sites per unit volume than the Cr hydrazide materials mentioned above.

Experimental Section

Chemicals were purchased from Aldrich and used as received. All experiments were performed under high purity Ar.

Preparation of $V(Mes)_3$·THF. To 50 mL of 1 M mesitylmagnesium bromide (MesMgBr) in tetrahydrofuran (THF) was added 33.33 mL of THF. Next, 6.22 g of VCl_3·3THF (97%) was added portion by portion. The obtained solution was stirred vigorously at room temperature for 2 h, after which a clear blue solution was obtained. To the solution was then added 21.66 mL of dioxane with stirring. After 2 h more, stirring was ceased and the solution was left to settle before filtering. The filtrate was collected and concentrated in vacuum until crystals formed. Next, 16.67 mL of diethyl ether was added, and the remaining product precipitated. The solid product was collected by filtration and washed several times with a solution of THF and ether (1:3 v/v) before drying in vacuum.[17]

Preparation of Anhydrous Hydrazine. Pure hydrazine was prepared from hydrazine monohydrate by azeotropic distillation with toluene to remove water and avoid possible explosion. First, 100 mL of hydrazine monohydrate and 250 mL of toluene were added to a 500 mL one-neck round-bottom flask, equipped with a thermometer to measure the gas temperature. A water condenser was connected and followed by two flashes to collect the waste liquid and dry hydrazine. The first step of distillation was carried out under argon and atmospheric pressure with water and toluene as products, which were collected at the first flash and removed at the end of this step. In the second step, 35 g of NaOH was added to the hydrazine−toluene flask, and the system was distilled under a vacuum. Pure hydrazine was collected in the second flash.[14b]

Preparation of A100 and A150 Vanadium Hydrazide Samples. The A100 sample was synthesized as follows: $V(Mes)_3$·THF (3.0 g, 6.24 mmol) was dissolved in 75 mL of dry toluene at room temperature in an Erlenmeyer flask, and then 0.15 mL of hydrazine (0.15 mL, 4.68 mmol) was added by syringe with vigorous stirring. The solution was stoppered, and stirring was continued for 12 h. The solution was then heated to 100 °C for 3 h with stirring. After this, the system was filtered, and a black solid was obtained. This solid was transferred to an air-free tube and put under a vacuum at room temperature for 12 h, followed by heating at 60 °C in vacuum for a period of 6 h, followed by another 6 h in vacuum at 100 °C. The A150 sample was obtained by continuing heating the A100 at 150 °C for 6 h in vacuum.

Preparation of B100 and B150 Samples. The same procedure was followed as with the A100 and A150 samples, but with 0.20 mL of hydrazine.

(5) (a) Kubas, G. J.; Ryan, R. R.; Swanson, B. I.; Vergamini, P. J.; Wasserman, H. J. *J. Am. Chem. Soc.* **1984**, *106*, 451. (b) Kubas, G. J. *Chem. Rev.* **2007**, *107*, 4152.
(6) Heinekey, D. M.; Lledós, A.; Lluch, J. M. *Chem. Soc. Rev.* **2004**, *33*, 175.
(7) Zhao, Y.; Kim, Y.; Dillon, A. C.; Heben, M. J.; Zhang, S. B. *Phys. Rev. Lett.* **2005**, *94*, 155504.
(8) Hoang, T. K. A.; Antonelli, D. M. *Adv. Mater.* **2009**, *21*, 1787.
(9) Heinekey, D. M.; Oldham, W. J., Jr. *Chem. Rev.* **1993**, *93*, 913.
(10) Yildirim, T.; Ciraci, S. *Phys. Rev. Lett.* **2005**, *94*, 175501.
(11) Dinca, M.; Dailly, A.; Liu, Y.; Brown, C. M.; Neumann, D. A.; Long, J. R. *J. Am. Chem. Soc.* **2006**, *128*, 16876.
(12) (a) Hamaed, A.; Trudeau, M.; Antonelli, D. M. *J. Am. Chem. Soc.* **2008**, *130*, 6992. (b) Hamaed, A.; Hoang, T. K. A.; Trudeau, M.; Antonelli, D. M. *J. Organomet. Chem.* **2009**, *694*, 2793.
(13) Hoang, T. K. A.; Hamaed, A.; Trudeau, M.; Antonelli, D. M. *J. Phys. Chem. C* **2009**, *113*, 17240–17246.
(14) (a) Fetter, N. R.; Bartocha, B. K. W. (U.S. Navy). U.S. Patent 3321503, April 3, 1962/May 23, 1967;*Chem. Abstr.* **1967**, *67*, 55828. (b) Schmidt, E. W. *Hydrazine and its Derivatives. Preparation, Properties, Application*; John Wiley & Sons, Inc.: New York, 2001; pp 99−105.
(15) Mai, H. V.; Hoang, T. K. A.; Hamaed, A.; Trudeau, M.; Antonelli, D. M. *Chem. Commun.* **2010**, *46*, 3206.
(16) Hamaed, A.; Mai, H. V.; Hoang, T. K. A.; Trudeau, M.; Antonelli, D. M. *J. Phys. Chem. C* **2010**, *114*, 8651.
(17) Seidel, V. W.; Kreisel, G. *Z. Anorg. Allg. Chem.* **1977**, *435*, 146.

Preparation of C100 and C150 Samples. The same procedure was followed as with the A100 and A150 samples, but with 0.30 mL of hydrazine.

Preparation of D100 and D150 Samples. The same procedure was followed as with the A100 and A150 samples, but with 0.40 mL of hydrazine.

Analysis. Powder X-ray diffraction (XRD) was performed on a Siemens D-500 diffractometer with Cu Kα radiation (40 kV, 40 mA) source. The step size was 0.02°, and the counting time was 0.3 s for each step. Diffraction patterns were recorded in the 2θ range 2.3−52°. Samples for XRD analysis were put in a sealed capillary glass tube to protect sample from air and moisture during the experiment.

Nitrogen adsorption and desorption data were collected on a Micromeritics ASAP 2010 instrument. All X-ray photoelectron spectroscopy (XPS) measurements were collected on samples prepared and loaded in a glovebox, using a Physical Electronics PHI-5500 spectrometer. Obtained data were referenced to the carbon C−(C,H) peak at 284.8 eV. Elemental analysis was performed by Galbraith Laboratories (Knoxville, TN).

Infrared spectroscopy was conducted using a Bruker Vector 22 instrument. In a typical experiment, 2 mg of sample was mixed with 500 mg of dry KBr, and a pellet was made in an inert atmosphere. The pellets were then transferred outside, and the measurements were conducted immediately.

Hydrogen Adsorption Measurements. Hydrogen adsorption isotherms were obtained by using a computer-controlled commercial gas reaction controller manufactured by Advanced Materials Corp. (Pittsburgh, PA). High-purity hydrogen (99.9995% purity) was used as the adsorbent. Hydrogen storage measurements on a standard AX-21 sample (4.5 wt %) were performed to ensure proper calibration and functioning of the instrumentation. Leak testing was also performed during each measurement by checking for soap bubbles at potential leak points. These measurements are necessary to ensure the veracity of the isotherms. In the H_2 adsorption−desorption experiments, complete reversibility was observed for all samples across the entire range of pressures. Samples were run at liquid nitrogen temperature (77 K), liquid argon temperature (87 K), and room temperature (298 K) to 85 bar. Isotherms were always measured first at room temperature and then at 77 or 87 K, and the temperature was kept constant by keeping the sample chamber in liquid N_2, liquid Ar, or water. The skeletal density was measured using a Quantachrome Ultrapycnometer. The bulk density was recorded on a benchtop density apparatus on finely ground powder samples of the materials. When the skeletal density is used for the gravimetric hydrogen uptake measurement, the compressed hydrogen within the pores is treated as part of the sample chamber volume. Therefore, only the hydrogen contained on or beneath the walls of the structure will be recorded by the pressure composition isotherm (PCI) instrument. This gravimetric value is termed the adsorption or excess storage. When the bulk density is used for this measurement, the hydrogen in the pores of the sample is automatically included in the calculation without any further correction, and the final value is termed the total storage[18] or absolute storage,[19] which represents all hydrogen contained in the sample, including the compressed gas in the voids and the hydrogen adsorbed on or beneath the walls of the structure. Gravimetric densities are recorded as read directly from the isotherms, while volumetric densities are calculated from the adsorption data and the skeletal or bulk density, depending on the desired value. The excess volumetric storage is typically calculated from the excess storage and the bulk density and gives a measure of the gas adsorbed on or in the solid phase of the material scaled across the entire volume occupied by the sample, including the void space. In materials such as metal−organic frameworks (MOFs) that possess a well-defined and constant ratio between mass and void space, this value is often quoted. For compressible materials that may have variable ratios of solid mass and void space, it can often help to scale the volumetric density to the solid phase alone, as the void space will vary on sample preparation. For this purpose, we define the true volumetric adsorption as the amount of hydrogen adsorbed on or in the solid portion of the sample. This is calculated from the excess storage data and the skeletal density. This value neglects the void space and is useful in comparing volumetric densities of ball-milled powders and gels to pure solid-phase materials such as metal hydrides. Since the materials in this study are between hydrides and physisorption materials in their mechanism of storage, this value is important. It also allows us to compare volumetric adsorption values of the solid phase alone from one sample to another without having to subtract out the void space. The absolute volumetric adsorption has also been defined[19] and is a representation of the sum of the excess volumetric storage plus the compressed gas in the void space. This can be calculated from the volumetric storage as measured from the instrument and the bulk density, or by taking the volumetric adsorption and adding on the amount in the void space calculated from the pore volume and the ideal gas law.[19] The first method is only possible when using the Advanced Materials instrument. In this paper we have chosen not to calculate this value (or the total gravimetric storage) because the differences between the skeletal densities and bulk densities are much smaller than in MOFs, and hence the void space contribution is negligible.

Enthalpies of adsorption were calculated using a variant of the Clapeyron−Clausius I equation taking both 77 and 87 K hydrogen excess storage data:

$$\ln\left(\frac{P_2}{P_1}\right) = -\Delta H_{ads}\frac{T_2 - T_1}{RT_2T_1} \quad (1)$$

where P_n is the pressure for isotherm n, T_n is the temperature for isotherm n, and R is the gas constant.

Pressure as a function of the amount adsorbed was determined by using exponential fits for each isotherm; the first 10−11 points of the isotherms were fit to the exponential equation. This exponential equation gives an accurate fit up to a pressure of 1 MPa, with the goodness of fit (R^2) above 0.99. The corresponding P_1 and P_2 values for a certain amount of H_2 adsorbed at both temperatures can be obtained from the simulated exponential equation. Using these numbers in eq 1, we then calculate the adsorption enthalpies.

EPR Experimental Details. Electron paramagnetic resonance (EPR) spectra were collected at room temperature using a Bruker EMXplus X-band (~9.4 GHz) spectrometer. Samples were placed in 4 mm outer-diameter quartz tubes sealed with O-ring needle valves. Sample volumes were ~300 μL. To produce hydrogen-loaded samples, hydrogen gas (grade 6) was applied directly, at a pressure of 1 atm, to the sample within the EPR tube using an airtight purge valve to ensure an inert environment.

Results and Discussions

Trimesitylvanadium(III) was reacted with varying ratios of anhydrous hydrazine in dry toluene. After 12 h of stirring, the reaction mixture was heated to 100 °C for 3 h, followed by filtration to obtain a black solid. This air- and moisture-sensitive material was heated in vacuum at 100 or 150 °C, and the resulting materials were named A100 and A150, respectively, for a $V(Mes)_3 \cdot THF/N_2H_4$ ratio of 4/3. Three other $V(Mes)_3 \cdot THF/N_2H_4$ ratios of 1/1, 2/3, and 1/2 were also employed, and those samples were named B100 and B150, C100 and C150, and D100 and D150, respectively. A possible mechanism for this reaction is shown in Figure 1.

The XRD patterns for the vanadium hydrazide materials heated at 150 °C in vacuum are shown in Figure S1 (Supporting

(18) Hu, X.; Skadtchenko, B. O.; Trudeau, M.; Antonelli, D. M. *J. Am. Chem. Soc.* **2006**, *128*, 11740.
(19) Furukawa, H.; Miller, M. A.; Yaghi, O. *J. Mater. Chem.* **2007**, *17*, 3197.

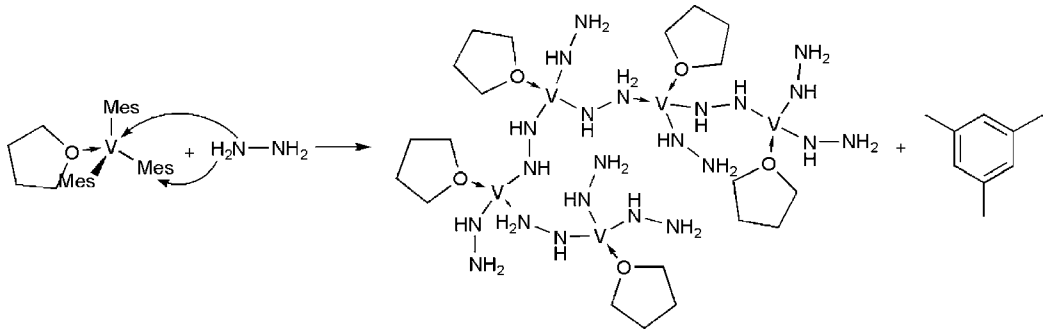

Figure 1. Possible mechanism for the reaction between $V(Mes)_3 \cdot THF$ and N_2H_4.

Table 1. C, H, N, and V Concentration of Vanadium Hydrazide Materials

sample	$V(Mes)_3 \cdot THF/N_2H_4$ ratio	vanadium (%)	carbon (%)	hydrogen (%)	nitrogen (%)
A150	4/3	37.00	13.58	2.46	10.54
B150	1/1	33.70	4.60	2.53	12.39
C150	2/3	52.25	4.01	1.87	16.60
D150	1/2	44.85	3.94	1.71	12.89

Information). All patterns were similar and exhibited a single broad reflection corresponding to a *d* spacing of 1.96 nm. The position of this reflection suggests nanoscopic periodicity, while the broadness of the reflection represents a lack of long-range order. Nitrogen adsorption isotherms recorded at 77 K are shown in Figure S2 (Supporting Information). These isotherms show a small amount of microporosity comprising ca. 20% the total volume adsorbed, with additional mesoporosity and textural porosity accounting for the remaining adsorption in roughly equal proportions, as evidenced by the slow rise between 0.2 and 0.8 P/P_0 and the sharp incline above 0.8 P/P_0, respectively. The specific surface areas of all materials decrease with increasing the drying temperature from 100 to 150 °C. For example, C100 possesses a Brunauer−Emmett−Teller (BET) surface area of 524 m^2/g, but after heating in vacuum to 150 °C, the surface area decreases to 348 m^2/g.

The C, H, N, and V elemental analysis data of vanadium hydrazide materials are shown in Table 1 and reflect the decreasing trend in carbon concentration with increasing hydrazine at 150 °C, from 13.58 to 3.94 wt %, consistent with a greater degree of elimination of arene with increased concentration of hydrazine. However, these carbon values are somewhat low due to carbide and nitride formation on combustion in the elemental analysis experiment, leading to less than 100% for all elements present. Drying at 150 °C leads to progressive arene elimination as monitored by IR spectroscopy (C−H stretch at 2850−2950 cm^{-1}), presumably by the thermally driven protolysis reaction between coordinated hydrazine and mesitylene groups. Aromatic C−C stretches are detected at 1589.62 and 1405.12 cm^{-1} in the spectrum of the C150 sample as well as C−O stretches for THF (962.15 cm^{-1}), confirming the presence of residual THF and mesitylene in this material (see Figure S13b in the Supporting Information).

XPS studies of the vanadium hydrazides were conducted, and the results are shown in Figures S3−S8 (Supporting Information). No charge neutralization was required, and emissions were observed at the Fermi level, suggesting that these materials are metallic. Multiple oxidation states of vanadium are detected in the vanadium 2p 1/2,3/2 region (Figures S4 and S5). By comparison with literature values, the emissions at 512.8 and 520.0 eV correspond to V(0),[20] the emissions at 513.8 and 520.9 eV can be assigned to a V(I) species,[21] and the emissions at 515.0 and 522.3 eV represent V(III),[22] while the emissions at 516.4 and 523.8 eV correspond to V(IV).[23] The appearance of multiple oxidation states both lower and higher than the V(III) starting material is consistent with disproportionation, common with vanadium. The XPS spectra of all materials in the N 1s region exhibit a broad emission centered at 396 eV with a shoulder at 398.5 eV which can be simulated as three major peaks (Figures S6 and S7). The first simulated emission, located at 395.6 eV, likely corresponds to an NH nitrogen bound directly to V.[24] The second emission, located at 396.4−396.6 eV, likely represents unbound terminal $-NH_2$ species,[25] while the third emission, located at 398 eV, can be assigned to a quaternary hydrazinium species bound to V.[26] The A150 sample has a low-intensity simulated peak at 398.8 eV, corresponding to a fourth nitrogen environment, possibly arising from a quaternary hydrazide nitrogen bound to V in a higher oxidation state than that from the emission at 398 eV.[27] There is also evidence for bound THF in the XPS from the oxygen region (Figure S8), as indicated by the high-intensity emissions centered at 530.4 eV.[28] The difficulty in removing THF is not surprising due to the well-documented high oxophilicity of early transition metals.

The excess storage isotherms of C100 and C150 samples are shown in Figure 2. At 77 K these isotherms show an initial rise at low pressure, consistent with a small amount of physisorption expected from the surface areas in the 242−524 m^2/g range, followed by a linear region which only begins to reach saturation in the D series of these samples (Table 2). At room temperature there is very little adsorption until 30 bar, after which a linear region emerges. Linear behavior without saturation is not typical of physisorption and suggests a different mechanism of hydrogen storage is operative in these materials. The gravimetric adsorption of the C150 sample is 1.17 wt % at 85 bar and 298 K,

(20) Franzen, H. F.; Sawatzky, G. *J. Solid State Chem.* **1975**, *15*, 229.
(21) Groenenboom, C. J.; Sawatzky, G.; Meijer, H. J. D.; Jellinek, F. *J. Organomet. Chem.* **1974**, *76*, C4–C6.
(22) Horvath, B.; Strutz, J.; Geyer-Lippmann, J.; Horvath, E. G. *Z. Anorg. Allg. Chem.* **1981**, *483*, 181.
(23) Kasperkiewicz, J.; Kovacich, J. A.; Lichtman, D. *J. Electron Spectrosc. Relat. Phenom.* **1983**, *32*, 123.
(24) Grunert, W.; Feldhaus, R.; Anders, K.; Shpiro, E. S.; Antoshin, G. V.; Minachev, Kh. M. *J. Electron Spectrosc. Relat. Phemon.* **1986**, *40*, 187.
(25) Kafizas, A.; Hyett, G.; Parkin, I. P. *J. Mater. Chem.* **2009**, *19*, 1399–1408.
(26) Lindberg, B.; Maripuu, R.; Siegbahn, K.; Larsson, R.; Golander, C.-G.; Erikkson, J. C. *J. Colloid Interface Sci.* **1983**, *95*, 308.
(27) Larkins, F. P.; Lubenfeld, A. *J. Electron Spectrosc. Relat. Phenom.* **1979**, *15*, 137–141, 1979.
(28) Yatsimirskii, K. B.; Nemoshalenko, V. V.; Aleshin, V. G.; Bratushko, Y. I.; Moiseenko, E. P. *Chem. Phys. Lett.* **1977**, *52*, 481.

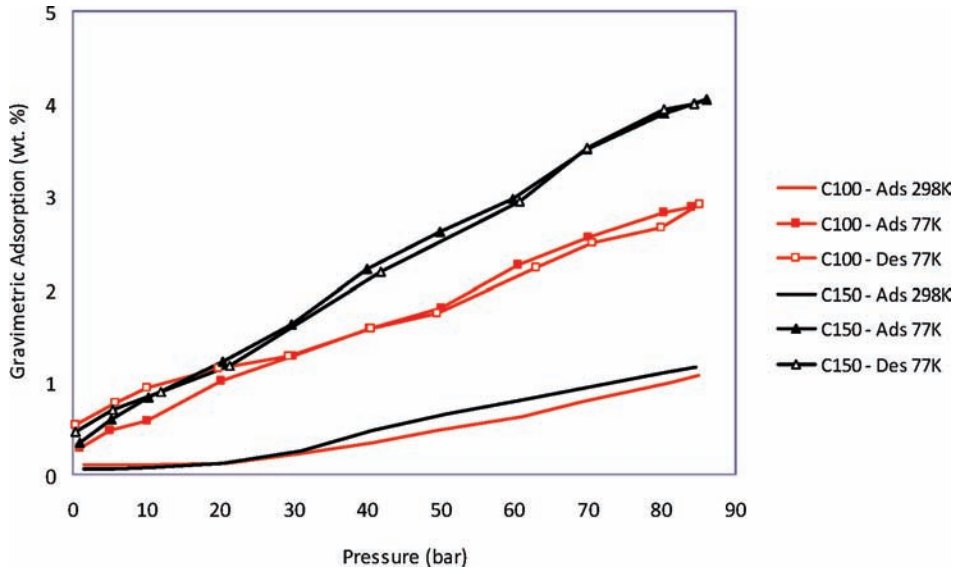

Figure 2. Hydrogen adsorption−desorption excess storage isotherms of C-series vanadium hydrazide materials synthesized with a vanadium:hydrazine ratio of 1:1.5.

Table 2. Summary of Excess Storage Results on Vanadium Hydrazide Materials and Carbon AX-21[a]

material	BET surface area (m^2/g)	skeletal density (g/cm^3)	gravimetric adsorption (wt %)	true volumetric adsorption (kg/m^3)	retention (%)
A100	268	1.9174	2.08 (at 77 K) 0.84 (at 298 K)	40 (at 77 K) 16.1 (at 298 K)	40
A150	242	2.3795	1.66 (at 77 K) 0.68 (at 298 K)	39.5 (at 77 K) 18.2 (at 298 K)	41
B100	378	2.1640	2.22 (at 77 K) 0.70 (at 298 K)	48 (at 77 K) 15.2 (at 298 K)	32
B150	329	2.2000	1.50 (at 77 K) 0.43 (at 298 K)	33 (at 77 K) 9.5 (at 298 K)	29
C100	524	2.1557	2.88 (at 77 K) 1.07 (at 298 K)	62 (at 77 K) 23.1 (at 298 K)	37
C150	348	1.9792	4.04 (at 77 K) 1.17 (at 298 K)	80 (at 77 K) 23.2 (at 298 K)	29
D100	307	2.0413	3.87 (at 77 K) 0.84 (at 298 K)	79 (at 77 K) 17.2 (at 298 K)	22
D150	256	2.4125	2.48 (at 77 K) 0.70 (at 298 K)	60 (at 77 K) 16.9 (at 298 K)	28
AX-21	3225	2.103	4.2 (at 77 K, 65 bar) 0.55 (at 298 K)	14 (at 77 K, 65 bar) –	13
MOF-5	3534		5.10 (at 77 K) 0.28 (at 298K)		5.5

[a] Data recorded at 85 bar.

while the true volumetric adsorption of this sample is 23.2 kg H_2/m^3 (see Experimental Section for a full explanation of volumetric capacities). This represents the amount of hydrogen contained in and on the surface of the solid portion of the sample without the compressed gas in the void space. For comparison, these values are over 3 times greater than those of compressed gas under the same conditions. At 77 K, this sample adsorbs 4.04 wt %, corresponding to a true volumetric adsorption of 80 kg H_2/m^3. Using the bulk density measured for this sample of 1.49 g/cm^3, excess volumetric storage capacities of 60.01 and 17.43 kg H_2/m^3 can be determined. These volumetric capacities at 77 K are in the range of the ultimate DOE goal of 70 kg/m^3, while the capacities measured at ambient temperature are close to the DOE 2010 goal of 28 kg/m^3. The volumetric performance of 60.01 kg H_2/m^3 is greater than that of MOF-177, which possesses a excess volumetric storage of 32.0 kg H_2/m^3 at 77 K and an absolute volumetric adsorption at 77 K of 49.0 kg H_2/m^3.[19] By comparing the gravimetric adsorption at 298 and 77 K, the retentions of excess adsorption capacities can be calculated and range from 41% to 22%. This is much higher than those of MOF-5 and carbons AX-21, which retain 5.5% and 13%, respectively, and once again suggests a different mechanism than simple physisorption. These results establish that a molar ratio of 1:1.5 and heating temperature of 150 °C is the optimal synthesis condition for hydrogen adsorption performance.

Further discussion on the relationship between the synthesis conditions and physical properties of these materials is useful. The elemental analysis results demonstrate that hydrazine ratios of 1:1 and 4:3 are not sufficient to remove enough alkyl groups to ensure high activity by reducing the steric profile around the metal center and lowering the system weight through substitution of mesitylene for hydrazine, but the highest ratio of 2:1 leads to a material in which saturation is reached at 80 bar. This is consistent with excess hydrazine blocking coordination sites that would otherwise be available for H_2. Heating these materials to 150 °C causes an increase in skeletal densities and decreases of gravimetric adsorption capacities of all samples except for

Table 3. Average Number of Hydrogen Molecules Adsorbed on Each Vanadium Site at 85 bar

	number of H_2/V	
sample	at 77 K	at 298 K
A150	1.14	0.47
B150	1.13	0.32
C150	1.96	0.57
D150	1.41	0.40

the C100 sample. The increase in density is likely due to the elimination of alkyl groups, a process that was monitored by observation of the C−H stretch in the IR spectrum. Heating at 150 °C also eliminates the adsorption−desorption hysteresis at 0−20 bar pressure observed in the samples heated to only 100 °C. This hysteretic effect also diminishes with decreasing $V(Mes)_3 \cdot THF/N_2H_4$ reaction ratio.

Calculations on the basis of gravimetric adsorption and the vanadium content in each sample result in an average number of hydrogen molecules per vanadium atom (Table 3) ranging from 1.13 to 1.96 H_2/V at 77 K and from 0.32 to 0.57 H_2/V at 298 K. The reason for the lower than expected number of active binding sites may be inhomogeneity in the hydrazide gel, which results in V(IV) and V(V) centers that do not bind H_2 and other V centers that may not be sterically accessible.

A 20-cycle run at 298 K with pressure up to 85 bar was carried out on the C150 sample. The results show no significant loss of excess adsorption capacity through cycling (Figure S12, Supporting Information). By fitting the adsorption isotherms at 77 and 87 K into the Clausius−Clapeyron equation, the isosteric heats of hydrogen adsorption can be calculated. The data for materials heated at 100 and 150 °C, as well as for carbon AX-21 as a standard, were measured under the same conditions (Figure 3). This isosteric heat of adsorption of all vanadium hydrazide materials rises from roughly 3−5 to 36.5 kJ/mol H_2, contrasting strongly to the behavior of AX-21, which has enthalpies that decrease from 6 to 3.3 kJ/mol H_2, typical of physisorption. The average value of the vanadium hydrazides falls in the range of 20−30 kJ/mol H_2, believed to be the ideal heat of hydrogen adsorption of suitable room-temperature hydrogen storage materials.[7] The rising enthalpies with surface coverage, observed in all previous publications from our group concerning hydrogen storage on supported low-coordinate, low-valent organometallic fragments, suggest a different adsorption mechanism, likely involving the Kubas interaction.[5,12,13] Rising enthalpies for Kubas-type hydrogen storage have been predicted in computations on hypothetical scandium-decorated bulkyballs, which show increasing binding energies for subsequent coordination of H_2 ligands from 0.30 eV for the first to 0.35 eV for the second and 0.42 eV for the third.[7]

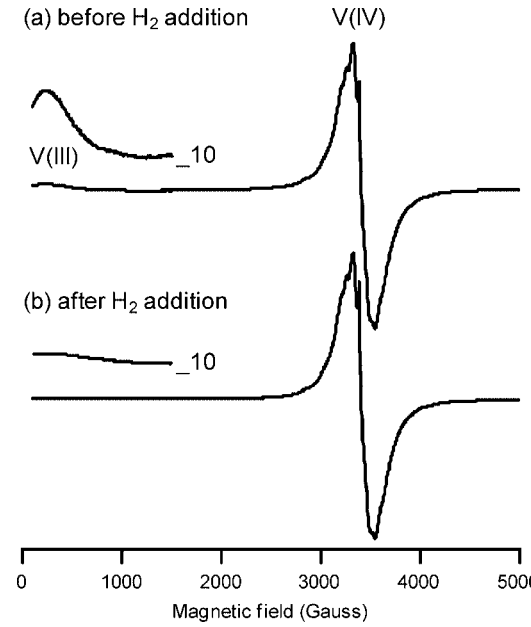

Figure 4. Room-temperature EPR spectra of vanadium hydrazide gel C150 (a) prior to exposure to hydrogen gas and (b) after exposure to hydrogen gas. Insets: low-field region magnified by a factor of 10. Experimental conditions: frequency, 9.382 GHz; microwave power, 20 mW; time constant, 20.48 ms; modulation amplitude, 10 G; average of three 45-s scans.

In order to further confirm Kubas binding in this system, EPR spectroscopic measurements were conducted on the C150 sample before and after hydrogen loading.[29] Prior to hydrogen addition, the X-band (9.4 GHz) EPR spectrum at room temperature showed a strong signal centered at 3411 G ($g = 1.96$), diagnostic of a V(IV) center ($3d^1$, $S = 1/2$), with characteristic partially resolved hyperfine splittings (51 V, $I = 7/2$, isotopic abundance = 99.75%) (Figure 4a).[29] A second paramagnetic species was also observed, exhibiting a broad, low-field peak

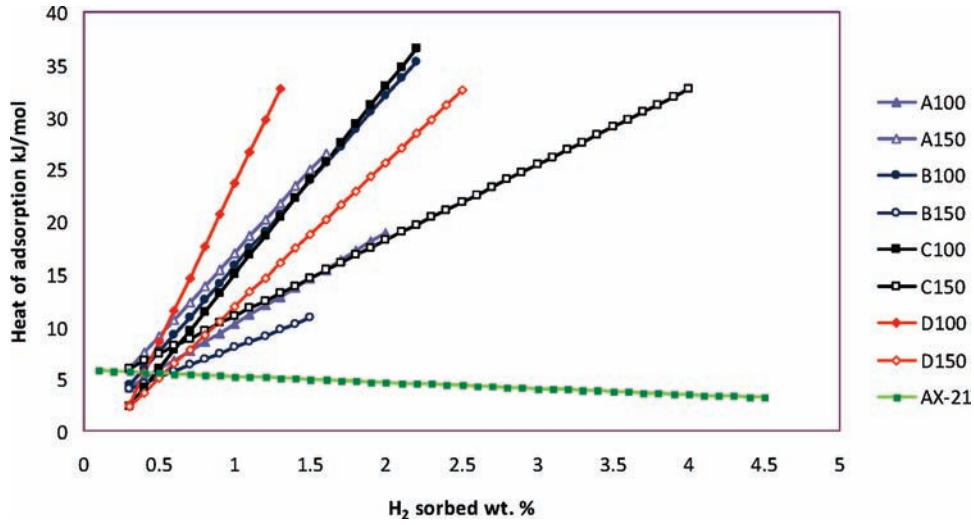

Figure 3. Heat of hydrogen adsorption on vanadium hydrazide materials and carbon AX-21.

(270 G), corresponding to a V(III) center ($3d^2$, $S = 1$).[30] EPR measurements of such species have been reported relatively infrequently, due to difficulties in measuring spectra from V(III) "non-Kramers" integer spin systems. Commonly, the zero-field splitting (zfs) of V(III) complexes is much larger than the microwave quantum used in EPR experiments ($\sim$0.3 cm^{-1} for X-band EPR), so that normally allowed transitions (DMS = $\pm$1) are no longer within the field/frequency range of conventional spectrometers.[31,32] However, in high symmetry systems the zfs is relatively small, permitting normally allowed transitions to be observed, as in the experiments described here.[31] Due to the amorphous nature of this material, only a small fraction of the V(III) centers are of high enough symmetry to be observed, leading to a lower intensity than expected for this signal.[33] This explains why the XPS shows a much higher relative proportion of V(III) to V(IV) than the EPR. After hydrogen gas was added to the sample, the EPR signal from the V(III) species was reduced in intensity by $\sim$90% (Figure 4b). This observation is consistent with the lowering of symmetry at the V(III) center caused by hydrogen binding, which increases the zfs, resulting in a new "EPR-silent" species. Since very little hydrogen is adsorbed at ambient pressure, an on−off equilibrium favoring the gas phase under these conditions is clearly enough to perturb this signal on the EPR time scale. By contrast, the signal from the V(IV) center was unchanged in shape or intensity, indicating that hydrogen binding occurs preferentially with the vanadium ions in the 3+ oxidation state in C150. Removing the hydrogen leads to a restoration in the intensity of the signal for V(III). At 77 K this signal is still unresolved, but this is expected due to the greater quantity of H_2 bound to the V(III) under these conditions, leading to an even further loss of symmetry on the EPR time scale. These observations are consistent with weak and reversible chemisorption to the V(III) centers through the Kubas interaction.

Conclusions

Vanadium hydrazides constitute a new class of hydrogen storage materials distinct from hydrides or physisorption materials that can function at room temperature and use pressure as a toggle switch to load or release hydrogen with a minimal kinetic barrier. By extending this class of materials to other transition metals systems with even better propensity for Kubas binding and a greater concentration of open coordination sites, it is likely that even higher storage capacities will be realized. The moderate enthalpies involved are just enough to allow room-temperature binding while not so strong as to create heat management issues in the system. Furthermore, the pressures used in this study fall short of the 200 bar norm used in the hydrogen transport industry. Since saturation was not reached in many of the isotherms at 85 bar, it is likely that isotherms recorded at 200 bar will show even higher capacities. These materials can potentially be used under the same conditions as compressed gas, which is already the main method of hydrogen storage in prototypes, but with higher volumetric capacities. Since hydrogen storage has been identified as the key problem in realizing the widespread use of hydrogen as a fuel, this new class of materials may show applications in the implementation into actual vehicles and power systems.

Acknowledgment. Natural Science and Engineering Research Council of Canada and Chrysler of Canada are acknowledged for funding. Profs. Holger Eichhorn and Samuel Johnson are acknowledged for help in XRD measurements and comments.

Supporting Information Available: XRD, BET surface areas for all samples dried at 150 °C, and XPS measurements for V, O, and N; hydrogen adsorption isotherms at 77 and 298 K for A, B, and D sample series; IR spectroscopy of C150 sample and the $V(Mes)_3 \cdot THF$ precursor; and the cycling result of C150. This material is available free of charge via the Internet at http://pubs.acs.org.

JA104926H

(29) Weil, J. A.; Bolton, J. R. *Electron Paramagnetic Resonance: Elementary Theory and Practical Applications*, 2nd ed.; John Wiley & Sons Inc.: Hoboken, NJ, 2007.
(30) Abragam, A.; Bleaney, B. *Electron Paramagnetic Resonance of Transition Ions*; Oxford University Press: London, 1970.
(31) Krzystek, J.; Fiedler, A. T.; Sokol, J. J.; Ozarowski, A.; Zvyagin, S. A.; Brunold, T. C.; Long, J. R.; Brunel, L.-C.; Telser, J. *Inorg. Chem.* **2004**, *43*, 5645.
(32) Telser, J.; Wu, C.-C.; Chen, K.-Y.; Hsu, H.-F.; Smirnov, D.; Ozarowski, A.; Krzystek, J. *J. Inorg. Biochem.* **2009**, *103*, 487.
(33) Alonso, P. J.; Forniés, J.; García-Monforte, A.; Martín, A.; Menjón, B. *Chem. Comm.* **2001**, 2138.